THE JOURNAL OF BIOLOGICAL CHEMISTRY VOL. 285, NO. 51, pp. 39943–39952, December 17, 2010

Inhibition of Deoxyhypusine Synthase Enhances Islet β Cell Function and Survival in the Setting of Endoplasmic Reticulum Stress and Type 2 Diabetes*[S]

Received for publication, July 29, 2010, and in revised form, October 4, 2010 Published, JBC Papers in Press, October 18, 2010, DOI 10.1074/jbc.M110.170142

Reiesha D. Robbins[‡], Sarah A. Tersey[§], Takeshi Ogihara[§], Dhananjay Gupta[§], Thomas B. Farb[¶], James Ficorilli[¶], Krister Bokvist[¶], Bernhard Maier[§1], and Raghavendra G. Mirmira[§‖2]

From the [‡]Department of Pharmacology, University of Virginia, Charlottesville, Virginia 22904, the [§]Department of Pediatrics and the Herman B. Wells Center for Pediatric Research, Indiana University School of Medicine, Indianapolis, Indiana 46202, the [¶]Lilly Research Labs, Eli Lilly and Company, Indianapolis, Indiana 46285, and the [‖]Departments of Medicine and of Cellular and Integrative Physiology, Indiana University School of Medicine, Indianapolis, Indiana 46202

Islet β cell dysfunction resulting from inflammation, ER stress, and oxidative stress is a key determinant in the progression from insulin resistance to type 2 diabetes mellitus. It was recently shown that the enzyme deoxyhypusine synthase (DHS) promotes early cytokine-induced inflammation in the β cell. DHS catalyzes the conversion of lysine to hypusine, an amino acid that is unique to the translational elongation factor eIF5A. Here, we sought to determine whether DHS activity contributes to β cell dysfunction in models of type 2 diabetes in mice and β cell lines. A 2-week treatment of obese diabetic C57BLKS/J-db/db mice with the DHS inhibitor GC7 resulted in improved glucose tolerance, increased insulin release, and enhanced β cell mass. Thapsigargin treatment of β cells *in vitro* induces a picture of ER stress and apoptosis similar to that seen in *db/db* mice; in this setting, DHS inhibition led to a block in CHOP (CAAT/enhancer binding protein homologous protein) production despite >30-fold activation of *Chop* gene transcription. Blockage of CHOP translation resulted in reduction of downstream caspase-3 cleavage and near-complete protection of cells from apoptotic death. DHS inhibition appeared to prevent the cytoplasmic co-localization of eIF5A with the ER, possibly precluding the participation of eIF5A in translational elongation at ER-based ribosomes. We conclude that hypusination by DHS is required for the ongoing production of proteins, particularly CHOP, in response to ER stress in the β cell.

Obesity is increasing at a rapid rate worldwide, with estimates that place its prevalence at >300 million people. Obesity is perhaps the single greatest risk factor for the development of type 2 diabetes mellitus. The relationship between obesity and diabetes is complex, but it is apparent that a direct correlation exists between increasing visceral fat and insulin resistance (1–3). However, only ~30% of obese, insulin-resistant individuals have diabetes, suggesting that other factors superimposing upon obesity must confer additional risks (4). It is now clear that defects in insulin secretion at the level of the islet β cell are paramount in the transition from a normoglycemic, insulin-resistant state to frank diabetes (5), and it is postulated that underlying genetic defects at the level of the β cell differentiates those who develop diabetes from those who do not (6). Prospective clinical (7) and autopsy (8) studies show significant reductions in β cell function and mass, respectively, in the transition from obesity-induced insulin resistance to frank type 2 diabetes.

The causes of islet dysfunction and death in the setting of insulin resistance include hyperglycemia, hyperlipidemia, cytokines, and deposition of islet amyloid polypeptide (9, 10). All of these causes stimulate intersecting pathways within the islet that lead to oxidative stress, inflammation, and endoplasmic reticulum (ER)[3] stress. These stress pathways are closely intertwined, such that activators of primarily one pathway acutely (*e.g.* cytokines causing inflammation or hyperglycemia causing oxidative stress) can evoke the other pathways chronically. Thus, drugs that show efficacy in any of these pathways (such as PPARγ agonists (11) and antioxidants (12)) may serve to globally reduce β cell stress in type 2 diabetes.

Recent studies have identified the enzyme deoxyhypusine synthase (DHS) and its substrate protein, eukaryotic translation initiation factor 5A1 (eIF5A1), as targets for reducing inflammation and related stress responses in a variety of cell types, including β cells (13, 14). DHS catalyzes the rate-limiting step in the post-translational synthesis of the polyamine-derived amino acid hypusine. Curiously, the only known proteins to contain hypusine in eukaryotic cells are eIF5A1 and eIF5A2 (15). Islet β cells contain only eIF5A1, which is a 17-kDa RNA binding protein that is required for G_1/S cell cycle progression and certain stress responses (13, 16).

* This work was supported, in whole or in part, by National Institutes of Health Grants R01 DK60581 (to R. G. M.) and F31 DK079420 (to R. D. R.). This work was also supported by a grant from the Ball Brothers Foundation (to R. G. M.).

[S] The on-line version of this article (available at http://www.jbc.org) contains supplemental Figs. S1 and S2.

[1] To whom correspondence may be addressed: Indiana University School of Medicine, 635 Barnhill Drive, MS2021, Indianapolis, IN 46202. Tel.: 317-278-8940; Fax: 317-274-4107; E-mail: bfmaier@iupui.edu.

[2] To whom correspondence may be addressed: Indiana University School of Medicine, 635 Barnhill Drive, MS2031, Indianapolis, IN 46202. Tel.: 317-274-4145; Fax: 317-274-4107; E-mail: rmirmira@iupui.edu.

[3] The abbreviations used are: ER, endoplasmic reticulum; eIF5A^{Hyp}, hypusinated eIF5A; DHS, deoxyhypusine synthase; RFP, red fluorescent protein; GTT, glucose tolerance test; Tg, thapsigargin; UPR, unfolded protein response; PI, propidium iodide; GC7, N1-guanyl-1,7-diaminoheptane; AUC, area under the curve.

siRNA-mediated depletion of eIF5A1 protected pancreatic islets from cytokine-induced inflammation *in vitro* and preserved glycemic control in the streptozotocin inflammatory model of diabetes in mice *in vivo*, in both cases by blocking the apparent translation of the *Nos2* gene encoding inducible nitric oxide synthase. Importantly, these effects were phenocopied when islets or whole animals were treated with N1-guanyl-1,7-diaminoheptane (GC7), a drug that inhibits DHS (13). These and other studies (17–19) suggest that the hypusine modification of eIF5A1 is crucial for its function as a translational factor for certain stress-induced mRNAs.

In this study, we sought to determine whether DHS plays a permissive role in the progression of islet dysfunction as seen in models of type 2 diabetes. We demonstrate that hypusination of eIF5A is maintained in islets of obese mice that are prone to diabetes but not in obese mice that are resistant to diabetes. Pharmacological inhibition of DHS improves insulin secretion and glucose tolerance in these diabetic mice. Experiments using INS-1 (832/13) β cells *in vitro* suggest that DHS activity via hypusinated eIF5A is important in ER stress-induced CHOP production and cellular apoptosis. Our findings reveal a heretofore unappreciated role for DHS and hypusinated eIF5A in the islet ER stress response and point to DHS as a potential therapeutic target in type 2 diabetes.

MATERIALS AND METHODS

Animal and Cell Culture Studies—Male *C57BLKS/J-db/db* mice, *C57BL6/J-db/db* mice, and their lean (*db/+*) littermate controls were purchased from The Jackson Laboratory at 8 weeks of age and maintained under protocols approved by the Indiana University School of Medicine Animal Care and Use Committee and Lilly Research Labs. Mice were treated with either saline control or GC7 at a dose of 4 mg/kg body weight via daily intraperitoneal injection as described previously (13). Treatment was initiated at 8–12 weeks of age and continued for 14 days. Intraperitoneal glucose tolerance tests (GTTs) using 0.1–1 mg/kg glucose and insulin tolerance tests using 3 units/kg insulin intraperitoneally were performed as described previously (11). Blood glucose concentrations were measured using a handheld glucometer (Abbott).

The rat insulinoma cell line INS-1 (832/13) was maintained as described previously (20). Mouse islets were isolated from pancreases as described previously (21) and then hand picked and cultured in RPMI medium (11 mM glucose) overnight prior to use.

Thapsigargin (Tg) and GC7 Incubations—Tg was dissolved in dimethyl sulfoxide and added to INS-1 (832/13) cell cultures at a final concentration of 1 μM. Unless otherwise stated, cells were incubated with Tg for 6 h at 37 °C. GC7 was prepared at a stock concentrations in 10 mM acetic acid and applied to cultures of 1×10^6 INS-1 (832/13) cells to obtain the final concentrations indicated. Hypusination assays using [^{3}H]spermidine in INS-1 (832/13) cells, and primary islets were conducted as described previously (13).

Hypusination Assays in Vitro—Ten ng of recombinant eIF5A protein (Prospec Bio) was added in a 20-μl reaction (50 mM glycine (pH 8.3), 20% glycerol, 2 mM dithiothreitol, 150 mM KCl, 10 mM $MgCl_2$, 0.1 mM NAD, 0.1 mg/ml bovine serum albumin) containing 2.0 μCi of [^{3}H]spermidine and 5 μg of nuclear or cytoplasmic extracts (prepared as previously described in Ref. 22, with NaCl concentrations normalized to 160 mM) from untreated or Tg-treated INS-1 (832/13) cells. Reactions proceeded for 60 min at 37 °C and were then terminated by addition of SDS gel loading buffer. Reactions were resolved on a 12% SDS- polyacrylamide gel and then visualized by fluorography.

Immunofluorescence Studies—The cDNA encoding DHS was obtained by PCR cloning from vector pCMV6-XL5.DHPS (Origene), subcloned into the CMV promoter-driven vector pEGFP (Clontech), and verified by automated sequencing. A red fluorescent protein (RFP)-tagged calreticulin expression vector (Origene) was used to mark the endoplasmic reticulum. pEGFP-eIF5A, pEGFP-eIF5A(K50A) (13), pEGFP-DHPS, and RFP-calreticulin vector were transfected into INS-1 (832/13) using Lipofectamine 2000 (Invitrogen) according to the manufacturer's protocol. Immunofluorescence of INS-1 (832/13) cells proceeded by direct visualization of GFP and RFP fusion proteins at 488 and 580 nm excitations, respectively. Cells were counterstained with DAPI to visualize nuclei (excitation, 380 nm) and then imaged using an Axio-Observer Z1 (Zeiss) inverted fluorescent microscope equipped with an Orca ER CCD camera (Hamamatsu).

Flow Cytometry—For flow cytometry studies, INS-1 (832/13) cells (adherent and floating) were collected and stained with propidium iodide (PI) and annexin V-FITC according to the manufacturer's protocol (BioVision). Approximately 30,000 cells per sample were subjected to flow cytometric analysis using a FACSCalibur (BD Biosciences) instrument to analyze the percent of FITC binding (excitation, 488 nm; emission, 530 nm) using an FITC signal detector (FL1) and percent PI staining by the phycoerythrin emission signal detector (FL2).

Real-time RT-PCR—Total RNA (5 ug) from islets or INS-1 (832/13) cells was reverse-transcribed, and the resulting cDNA was subjected to quantitative PCR using SYBR Green I-based technology and specific primers. Primers for *Ins-1/2* and *Ins-2* pre-mRNA were described previously (23). Components of the ER stress pathway in mouse (total *Xbp1*, spliced *Xbp1*, and *Chop*) and rat (total *Xbp1* and spliced *Xbp1*) were amplified with primers and cycling parameters described previously (24). Taqman® probes (Applied Biosystems) were used to amplify all other genes from rat (*Actb*, *Gpx1*, *Grp94*, *Ucp2*, *Slc2a2*, *Atf4*, *Atf6*, *Pdx1*, *Gck*, PPARγ, *Igf1*, *Kcnj11*, *Chop*, *Iapp*, and *Ptpn2*). The threshold cycle (C_T) methodology was used to calculate relative quantities of mRNA products from each sample, and all samples were corrected for total RNA by normalizing C_T values to the C_T value of *Actb* message. All data represent the average of triplicate determinations from at least three independent experiments.

Immunoblot Analysis—Whole cell extracts were resolved by electrophoresis on a 4–20% SDS-polyacrylamide gel, followed by immunoblot using monoclonal anti-eIF5A1 (BD Bioscience), monoclonal anti-β actin (clone C4) (MP Biomedicals), monoclonal anti-CHOP (Santa Cruz Biotechnology

or Affinity Bioreagents), polyclonal anti-ATF4 (Santa Cruz Biotechnology), polyclonal anti-eIF2-α (Cell Signaling), polyclonal antiphospho-eIF2-α (Cell Signaling), and anti-total and cleaved caspase-3 (Cell Signaling) primary antibodies and IRDye 800 or IRDye 700 fluorophore-labeled secondary antibodies (Li-Cor Biosciences). Immunoblots were visualized using the Li-Cor Odyssey system (Li-Cor Biosciences).

siRNA Studies—For siRNA-mediated knockdown experiments, 1×10^6 INS1 cells (832/13) were transfected with a SMARTpool of siRNA duplexes (50 nM) against rat eIF5A1 (catalog no. L-083885-01; Dharmacon) or siGenome nontargeting siRNA 1 (catalog no. D-001210-01-05; Dharmacon), using DharmaFECT 1 transfection reagent (Dharmacon) as described previously (13).

Hormone Measurements—Two-site immunospecific ELISA kits (ALPCO Diagnostics) were used to measure insulin and proinsulin from mouse serum and from acid ethanol-extracted total protein from INS-1 (832/13) cells according to the manufacturer's protocol. All data represent the average of three independent experiments.

Statistics—Data are shown as mean ± S.E. One-way ANOVA (with Bonferroni's post test) was used for comparisons involving >two conditions, and a two-tailed Student's *t* test was used for comparisons involving two conditions. GraphPad Prism (version 5.0) software was used for all statistical analyses. p values < 0.05 were considered significant.

RESULTS

Hypusination Activity in Diabetic Islets—Prior studies demonstrated that hypusinated eIF5A (eIF5A^{Hyp}) and the activity of its hypusinating enzyme DHS contribute to inflammatory signaling and dysfunction in pancreatic islets (13). To determine whether the rate of hypusination correlates with islet dysfunction in the setting of type 2 diabetes, we studied two obese stains of mice (*C57BL6/J-db/db* and *C57BLKS/J-db/db*) that harbor homozygous truncations in the leptin receptor but exhibit differing degrees of metabolic control and islet function. As shown in Fig. 1, *A* and *B*, both *C57BL6/J-db/db* and *C57BLKS/J-db/db* strains display comparable and significantly greater body weights compared with their lean (*db/+*) littermate controls, but only the *C57BLKS/J-db/db* strain demonstrates fasting hyperglycemia consistent with diabetes (mean blood glucose 250 mg/dl). In intraperitoneal GTTs, lean littermate controls of both strains exhibit identical glucose tolerance (Fig. 1*C*), whereas *C57BLKS/J-db/db* mice demonstrate significantly worse glucose tolerance compared with *C57BL6/J-db/db* mice (Fig. 1*D*). Prior studies suggest that differences in β cell insulin secretion largely underlie this difference in metabolic control between the two mouse strains (25, 26).

To determine whether differences in hypusination activity correlates with differences in islet dysfunction between the two *db/db* strains, we next isolated islets from animals and performed a 4-h pulse with [^{3}H]spermidine to look at the rate of formation of eIF5A^{Hyp}. Fig. 1*E* demonstrates that, compared with *db/+* controls, normoglycemic *C57BL6/J-db/db* mice show a reduction of eIF5A hypusination activity, as judged by the ratio of [^{3}H]eIF5A^{Hyp}:total eIF5A, whereas diabetic *C57BLKS/J-db/db* mice exhibit hypusination activity that is comparable to controls. These data raise the intriguing possibility that down-regulation of hypusination activity in islets may be important, in part, for the maintenance of islet function and normoglycemia (as seen in *C57BL6/J-db/db* mice), whereas unmitigated hypusination activity (as seen in

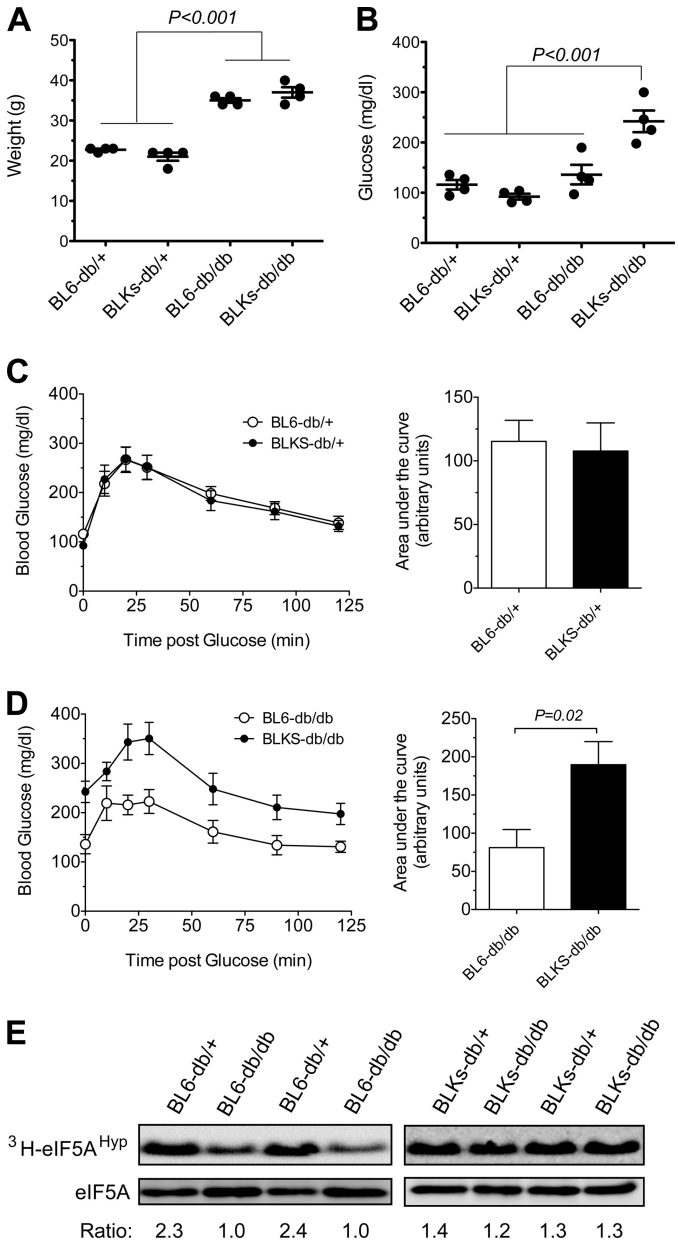

FIGURE 1. **Glucose homeostasis and islet eIF5A hypusination levels in control and diabetic mice.** Obese 12-week-old *C57BL6/J-db/db* (*BL6-db/db*) and *C57BLKS/J-db/db* (*BLKS-db/db*) mice and lean littermate *C57BL6/J-db/+* (*BL6-db/+*) and *C57BLKS/J-db/+* (*BLKS-db/+*) were studied for glucose homeostasis and islet eIF5A hypusination levels. *A*, body weights of mice; *B*, results of fasting blood glucoses; *C*, results of GTTs (1 mg/kg glucose given intraperitoneally) and corresponding AUC analysis of GTTs for *BL6-db/+* and *BLKS-db/+* mice; *D*, results of GTTs (0.25 mg/kg glucose given intraperitoneally) and corresponding AUC analysis of GTTs for *BL6-db/db* and *BLKS-db/db* mice; *E*, PAGE showing results of hypusination assays *in vitro* using [^{3}H]spermidine and isolated islets from mice and immunoblots from the same protein isolates for total eIF5A protein. Ratios at the *bottom of the panel* indicate the intensity of the [^{3}H]eIF5A^{Hyp} signal to the intensity of the total eIF5A protein signal. Data are presented as mean ± S.E.

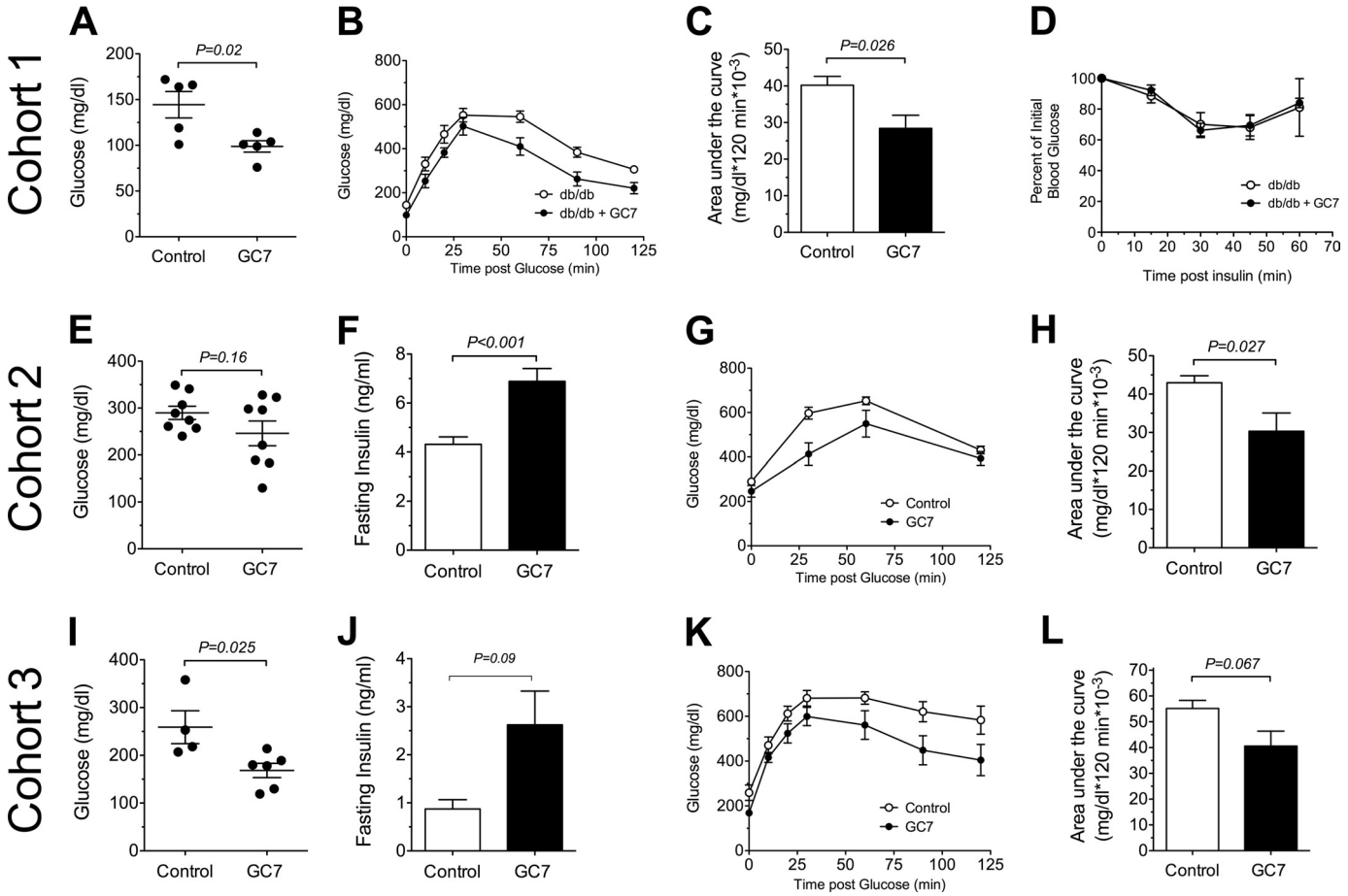

FIGURE 2. **Glucose homeostasis in obese diabetic mice receiving GC7, an inhibitor of DHS.** Three cohorts of *C57BLKS/J-db/db* mice ($n = 6–8$ per group), aged 8–12 weeks, received 4 mg/kg GC7 (or saline control) intraperitoneally for 14 days. *A–D*, results of fasting blood glucose (*A*), GTTs (1 mg/kg glucose injection) (*B*), AUC for the GTTs (*C*), and insulin tolerance tests (*D*) in cohort 1. *E–H*, results of fasting blood glucose (*E*), fasting plasma insulin (*F*), GTTs (0.1 mg/kg glucose injection) (*G*), and AUC for the GTTs (*H*) in cohort 2. *I–L*, results of fasting blood glucose (*I*), fasting plasma insulin (*J*), GTTs (0.25 mg/kg glucose injection) (*K*), and AUC for the GTTs (*L*) in cohort 3. Data are presented as mean ± S.E.

C57BLKS/J-db/db mice) may contribute negatively to islet function and glycemic control.

DHS Inhibition Improves Glycemic Control, Insulin Release, and Islet Mass in Diabetic Mice—To assess whether inhibition of hypusination improves islet function and metabolic control in the setting of obesity-related diabetes, we subjected 8–12-week-old *C57BLKS/J-db/db* mice to daily intraperitoneal injections of 4 mg/kg of the DHS inhibitor GC7 or control saline. In prior studies, we showed that GC7 at this dose led to inhibition of hypusination activity, as judged by substantial reductions in the rate of $eIF5A^{Hyp}$ formation in isolated islets (13). We treated three separate cohorts of animals for 2 weeks: cohort 1 underwent GTTs (1 mg/kg glucose given intraperitoneally) and insulin tolerance tests (Fig. 2, *A–D*), cohort 2 underwent GTTs (0.1 mg/kg glucose given intraperitoneally) and analysis of serum insulin levels (Fig. 2, *E–H*), and cohort 3 underwent GTTs (0.25 mg/kg glucose given intraperitoneally), analysis of serum insulin levels, and immunohistochemical analysis of pancreases (Fig. 2, *I–L*, and Fig. 3). Importantly, the animals that received GC7 did not exhibit any differences in food consumption or weight gain compared with control animals during the 2-week period (data not shown). In all cohorts, the animals that received GC7 exhibited significant or near-significant reductions in fasting blood glucoses (Fig. 2, *A*, *E*, and *I*), which were correlated to increased fasting serum insulin levels (Fig. 2, *F* and *J*). Insulin tolerance was unchanged by GC7 treatment, as observed in cohort 1 (Fig. 2*D*). GTTs in all cohorts of GC7-treated animals showed improved glucose clearance, as judged by an area-under-the-curve analysis (Fig. 2, *B*, *C*, *G*, *H*, *K*, and *L*). Taken together, the data in Fig. 2 suggest that the improved glycemic control following DHS inhibition by GC7 arose from improvements in insulin secretion.

To determine whether this improved insulin secretion correlated with improvements in β cell mass, we next performed islet morphometry using pancreases from cohort 3 and *C57BLKS/J-db/+* lean littermates. As shown in the representative immunohistochemical stain in Fig. 3*A*, animals receiving GC7 demonstrated apparently larger islets compared with both untreated *C57BLKS/J-db/db* control and *C57BLKS/J-db/+* lean littermates. β cell mass, as determined by morphometry of insulin-positive cells, was significantly greater in GC7-treated animals (Fig. 3*B*). Interestingly, the increased β cell mass in treated animals was correlated to a reduction in the fasting serum proinsulin:insulin ratio compared with untreated controls (Fig. 3*C*); this ratio has been suggested to re-

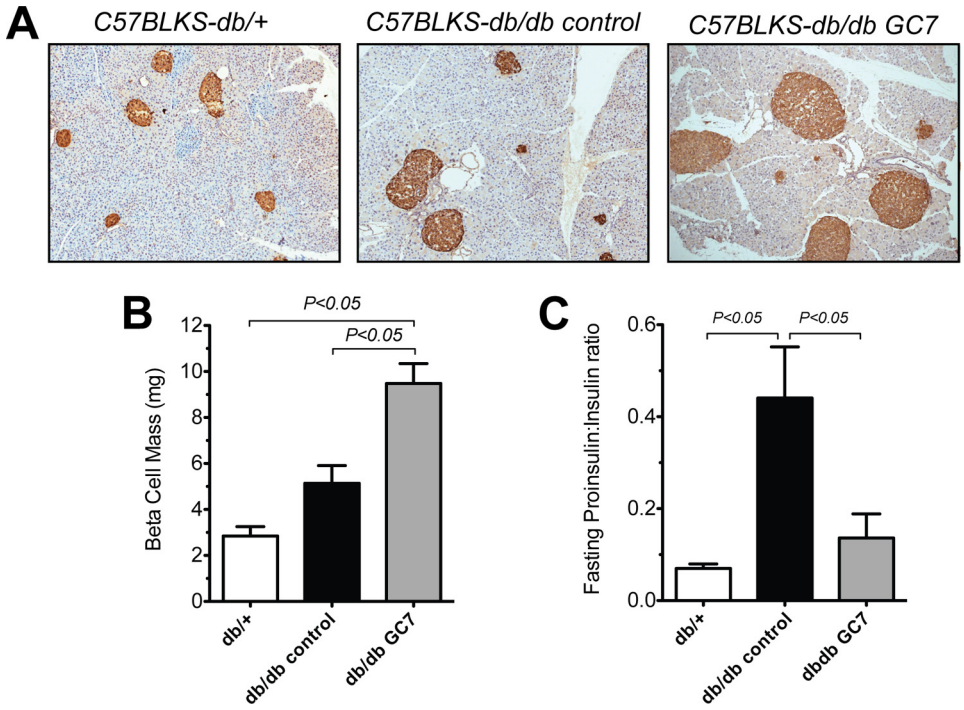

FIGURE 3. **β cell mass and plasma hormone ratios in mice receiving GC7, an inhibitor of DHS.** *C57BLKS/J-db/db* mice (*db/db*) from cohort 3 (see Fig. 2) and control, age-matched lean *C57BLKS/J-db/+* littermates (*db/+*) were euthanized after an overnight fast, and pancreases and plasma were collected. *A*, representative pancreas sections from the indicated mice stained for insulin (*brown*) and counterstained with hematoxylin (*blue*). Islet β cells are stained brown (original magnification, ×200); *B*, results of morphometric analysis of β cell mass from the indicated mice. For mass determination, a minimum of three pancreatic sections taken 75 μm apart from three mice per group were quantitated as described under "Materials and Methods." *C*, results of plasma proinsulin:insulin ratios from fasted mice in cohort 3.

flect ER capacity to properly fold and process proinsulin via the enzyme PC1/3, with higher ratios suggestive of a defect (27–31). These results suggest that inhibition of DHS preserves islet function and mass in the setting of obesity-related diabetes, possibly through effects on ER folding and processing capacity.

DHS Inhibition Does Not Prevent UPR, but Blocks ER Stress-induced Activation of Hypusination and Prevents CHOP Production—To identify mechanisms by which DHS inhibition preserves islet mass and function, we utilized a cell model system *in vitro* that has been shown to mimic β cell dysfunction in *db/db* mice. INS-1 (832/13) cells treated with 1 μM thapsigargin (Tg) exhibit ER stress and defects in intracellular calcium homeostasis similar to those seen in islets from diabetic *db/db* mice (11, 32). Tg is an inhibitor of the sarco-endoplasmic reticulum Ca^{2+} ATPase, and causes the rapid activation of the unfolded protein response (UPR) as observed in ER stress. Fig. 4*A* shows that treatment with 1 μM Tg for 6 h results in an increase in the proinsulin:insulin ratio in INS-1 (832/13) cells, similar to that observed in the serum of *C57BLKS/J-db/db* mice (Fig. 3*C*). Interestingly, this altered proinsulin:insulin ratio in the presence of Tg correlates with an increase in hypusination activity, as shown in Fig. 4*B*. A 1 h pretreatment with 100 μM GC7 prevents the increase in both hypusination (Fig. 4*B*) and the proinsulin:insulin ratio (Fig. 4*A*) in response to Tg. The Tg-induced increase in hypusination activity was not accompanied by any change in the level of the rate-limiting enzyme DHS (immunoblot in Fig. 4*B*), suggesting that the acute changes in hypusination rates likely result from increases in DHS activity rather than protein levels.

To ascertain the effect of DHS inhibition on the UPR induced by Tg, we next incubated INS-1 (832/13) cells with Tg or Tg plus GC7 and examined markers of the UPR. As shown in Fig. 4*C*, Tg treatment for 6 h resulted in the induction of the mRNAs for ER stress-responsive genes (*Chop*, *Xbp1*, spliced *Xbp1*, *Atf4*, *Atf6*, and *Grp94*) and antioxidative genes (*Gpx1*, *Ucp2*, and PPARγ), all of which are characteristic of UPR activation as seen in mouse models of ER stress (33). Genes for β cell-specific mRNAs showed no substantial changes with Tg treatment, except for the short half-life species pre-mRNA encoding preproinsulin (*pre-Ins2*) (23), which was reduced almost 100-fold and is reflective of the acute shut down of insulin gene transcription in the setting of the UPR (supplemental Fig. S1*A*). Treatment with both Tg and GC7 led to mRNA changes that were comparable with those of Tg alone (Fig. 4*C* and supplemental Fig. S1*A*), suggesting that GC7 does not affect substantially the transcriptional responses of the UPR.

We next examined the protein responses to Tg and Tg plus GC7 treatments, as shown in the immunoblots in Fig. 5*A*. Tg led to a rapid (within 2 h) induction of eIF2-α phosphorylation and minimal or no increase in ATF4 protein, both of which were unaffected by concurrent GC7 treatment. There was no discernible induction of inducible nitric oxide synthase in these studies (data not shown). However, whereas Tg treatment led to a rapid (within 2 h) induction of CHOP, concurrent treatment with GC7 blocked this increase in CHOP.

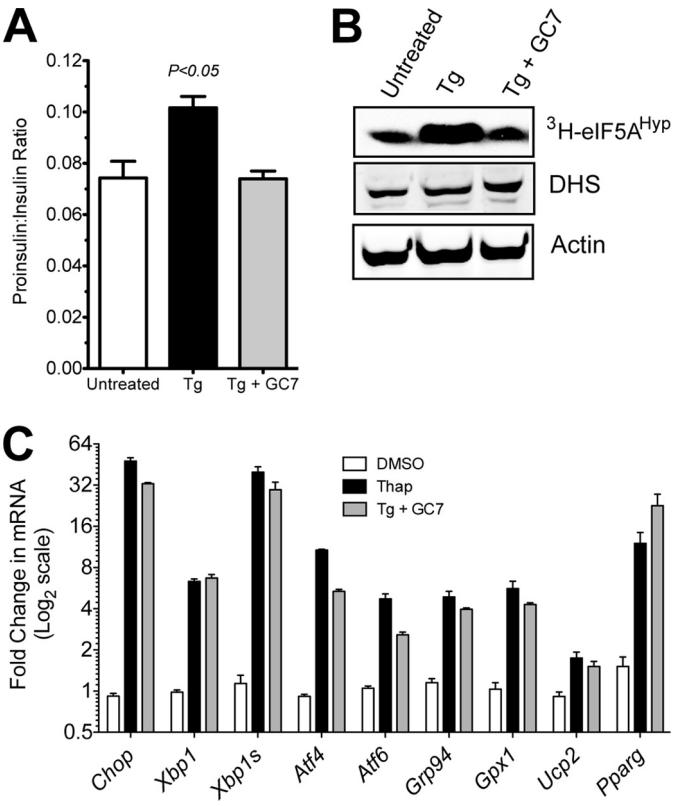

FIGURE 4. **Tg treatment of INS-1 (832/13) β cells increases hypusination activity and up-regulates UPR genes.** INS-1 (832/13) cells were untreated or treated with 1 μM Tg for 6 h or 1 μM Tg for 6 h plus 100 μM GC7 (added 1 h before Tg) (*Tg+GC7*). *A*, results of cellular proinsulin:insulin ratio from INS-1 (832/13) cellular extract; *B*, hypusination assay using [^{3}H]spermidine (*top panels*) and immunoblot for total DHS and actin levels (*bottom two panels*); *C*, results of real-time RT-PCR for UPR genes. Data in *A* and *C* represent the results from three independent experiments. *DMSO*, dimethyl sulfoxide.

To determine whether GC7 might have led to an increase in the rate of CHOP degradation (as opposed to a block in CHOP production), we performed studies using the proteasome inhibitor MG132. As shown in Fig. 5*B*, incubation of INS-1 (832/13) cells with MG132 alone led to an increase in CHOP protein, suggesting that proteasome pathways at least partially degrade endogenous CHOP protein. Incubation of cells with Tg+MG132+GC7 resulted in less CHOP protein induction than with either MG132 or with Tg+MG132. Assuming that MG132 resulted in complete inhibition of the proteasome pathway, these results increase the likelihood that GC7 blocks *Chop* mRNA translation rather than promotes CHOP protein degradation. Of significant interest, caspase-3 cleavage, a downstream effect of CHOP activity and a marker of cellular apoptosis, was also blocked by GC7 treatment. Dose-response experiments (Fig. 5*C*) showed that the inhibitory effects on CHOP and caspase-3 cleavage was evident at concentrations as low as 3 μM and reached a maximum apparent effect at 30 μM. Use of siRNA against eIF5A (si-eIF5A) in INS-1 (832/13) cells resulted in a reduction in caspase-3 cleavage in response to Tg similar to that observed with GC7 inhibition (Fig. 5*D*), reaffirming that the effects of DHS inhibition are closely tied to eIF5A function. In total, these results suggest that although activation of the UPR appears intact in the presence of DHS inhibition, there is impairment in the apparent translation of the mRNA encoding CHOP and the subsequent activation of the apoptotic pathway downstream of CHOP.

DHS Inhibition Protects β Cells against ER Stress-induced Apoptotic Death—To determine more directly whether the block in CHOP production resulted in protection from apoptotic death, we performed flow cytometry of INS-1 cells stained for annexin V-FITC and PI. Fig. 5*E* and supplemental Fig. S2*A* show that upon overnight treatment with Tg alone, 90% of cells undergo either early (annexin V^+/PI^-) or late (annexin V^+/PI^+) apoptosis. However, following a 1-h pretreatment with GC7, only 4–7% of cells underwent apoptosis in response to Tg, a finding that was comparable with untreated controls (Fig. 5*E* and supplemental Fig. S2, *B* and *C*). Notably, when GC7 was added 1 or more hours after Tg, there was progressively less protection against apoptosis (supplemental Fig. S2, *D–I*). On the one hand, this "lead time" that is necessary to observe the protective effect of GC7 may reflect the timing required to deplete sufficient endogenous $eIF5A^{Hyp}$ levels once DHS is inhibited (half-life of $eIF5A^{Hyp}$ in INS-1 (832/13) cells is 4–6 h (13)); on the other hand, it may simply reflect the need to inhibit CHOP induction in the earliest phases of the UPR to avoid cascades leading to cellular apoptosis.

Cytoplasmic Redistribution of eIF5A in Response to ER Stress Is Hypusine-dependent— eIF5A has been shown to have complex intracellular distributions, which likely reflect its compartment-specific activities that include nuclear-to-cytoplasmic shuttling of mRNAs and translational elongation at cytoplasmic ribosomes (13, 19, 34, 35). In prior studies, it was demonstrated that eIF5A localization shifts from a whole-cell distribution to a primarily cytoplasmic one in a hypusine-dependent manner in response to cytokine signaling (13). To determine whether intracellular localization of eIF5A is consistent with a more cytoplasmic role with respect to translation in response to ER stress, we transfected GFP-labeled eIF5A into INS-1 (832/13) β cells and examined its intracellular distribution in response to Tg treatment. As shown in Fig. 6*A*, GFP-eIF5A exhibited both cytoplasmic and nuclear distributions in untreated cells; upon treatment with Tg for 4 h, there was a significant shift of the protein into a primarily cytoplasmic distribution. This translocation phenomenon appears to be hypusine-dependent, as a mutant of eIF5A containing a Lys^{50}-to-Ala (K50A) substitution (that is incapable of being hypusinated) did not significantly redistribute in response to Tg (Fig. 6*A*). This finding suggested to us that compartment-specific hypusination in the nucleus may be occurring in response to ER stress. To test this possibility, we performed hypusination assays *in vitro* using nuclear and cytoplasmic fractions of INS-1 (832/13) cells, [^{3}H]spermidine, and purified eIF5A protein. As shown in Fig. 6*B*, cytoplasmic extracts demonstrate hypusination activity in INS-1 (832/13) cells, but activity in nuclear extracts is not discernible. However, treatment with Tg results in clear hypusination activity in nuclear extracts, suggesting that either a resident nuclear species of DHS is activated upon Tg treatment or that DHS becomes translocated to the nucleus upon Tg treatment. To

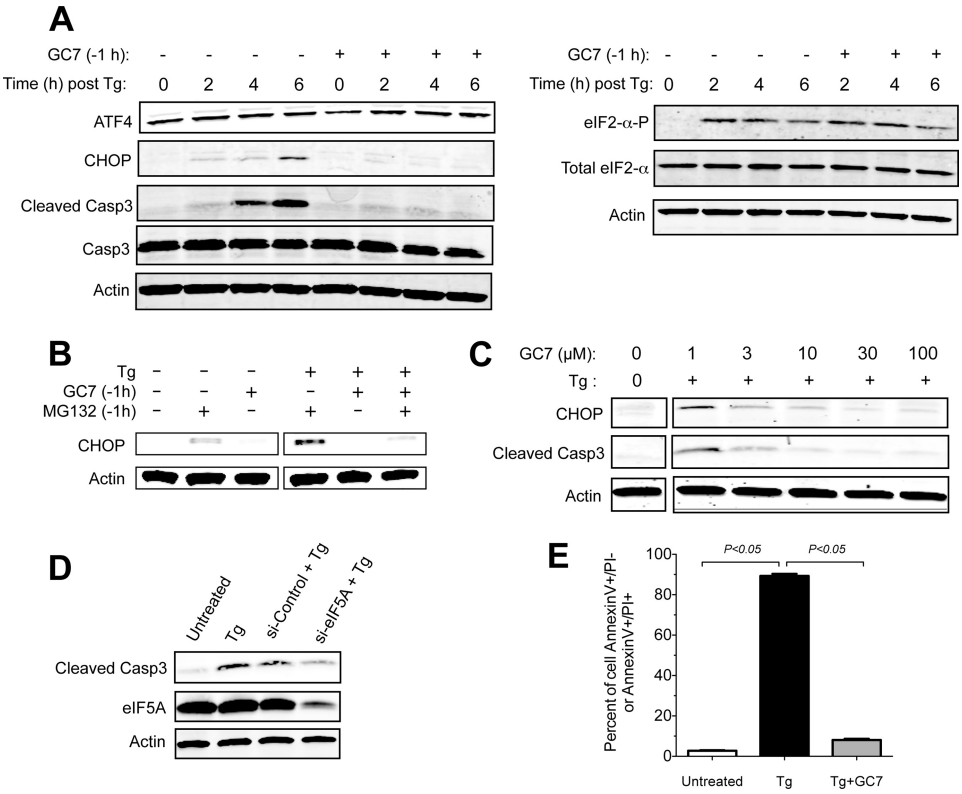

FIGURE 5. **DHS inhibition blocks CHOP and caspase-3 production and protects INS-1 (832/13) β cells from apoptotic death.** *A*, results of immunoblot analysis following treatment of INS-1 (832/13) cells with Tg (1 μM) for various times and/or GC7 (100 μM) added 1 h prior to Tg in the culture (−1 h). *B*, results of immunoblot analysis following treatment of INS-1 (832/13) cells for 6 h with Tg (1 μM), GC7 (100 μM), and/or MG132 (10 μM). *C*, results of immunoblot analysis following treatment of INS-1 (832/13) cells for 6 h with 1 μM Tg and the indicated concentrations of GC7. *D*, INS-1 (832/13) cells were transfected with no siRNA, control siRNA (*si-Control*), or siRNA against eIF5A (*si-eIF5A*) and then treated with Tg (1 μM) for 6 h, then subjected to the immunoblot analysis shown; *E*, results of annexin V-FITC/PI flow cytometry analysis of INS-1 (832/13) cell cultures untreated or treated with Tg (1 μM) overnight and with GC7 (10 μM) added 1 h prior to Tg. In *E*, data represent results from three independent experiments. *Casp3*, caspase-3.

assess the latter possibility, we transfected a vector encoding GFP-DHS into INS-1 (832/13) cells and then imaged the cells following Tg treatment. As shown in Fig. 6*A*, treatment with Tg leads to a significant translocation of DHS from the cytoplasm to the nucleus. These results suggest that stress conditions, such as those induced by Tg, appears to regulate cytoplasmic and nuclear compartmentation of not only eIF5A but also DHS.

Translation of mRNA is largely shifted to ER-bound ribosomes in the setting of ER stress (36); we therefore attempted to determine whether eIF5A localizes to markers of the ER under conditions of ER stress. INS-1 (832/13) cells were transfected with plasmids encoding GFP-eIF5A and RFP-labeled calreticulin (a calcium-binding protein associated with the ER), and co-localization of the two proteins was visualized in co-expressing cells. As shown in Fig. 6*C*, Tg-treated cells exhibited co-localization of GFP-eIF5A and RFP-calreticulin (as indicated by the yellow color in cells in Fig. 6*C*), whereas untreated cells showed no discernible co-localization. Concurrent treatment of INS-1 (832/13) cells with Tg plus the hypusination inhibitor GC7 inhibited the co-localization of GFP-eIF5A with RFP-calreticulin (Fig. 6*C*). Mutation of the hypusination target residue Lys^{50}-to-Ala (K50A) similarly blocked co-localization with RFP-calreticulin. These studies suggest that eIF5A exhibits hypusine-dependent co-localization with markers of the ER during the Tg-induced UPR.

DISCUSSION

Islet β cell dysfunction is now recognized as the hallmark of diabetes-prone obesity. Although genome-wide association studies have identified a number of β cell genes in humans that correlate with type 2 diabetes, such as *TCF7L2*, *HHEX,* and *SLC30A8* (6), it is still unclear how defects in the proteins encoded by these genes affect signaling pathways that are vital to β cell function. One of the pathways contributing to β cell dysfunction is ER stress (37, 38). The ER is a highly organized organelle responsible for the translation and proper folding of secreted proteins such as insulin. As such, the ER is central to the function of the β cell, which relies exclusively upon this organelle to produce and fold proinsulin for its eventual processing and secretion. When ER protein load is increased, as in the setting of obesity and insulin resistance, pathways are stimulated (collectively known as the unfolded protein response, or UPR) that serve to reduce the ER load by inhibiting translation and activating molecular chaperones and catalysts to enhance protein folding (39). The *db/db* mouse model of diabetic obesity, particularly on the *C57BLKS/J* background, exhibits features of islet ER stress; knock-out of the *Chop* gene on the *db/db* background preserves both islet mass

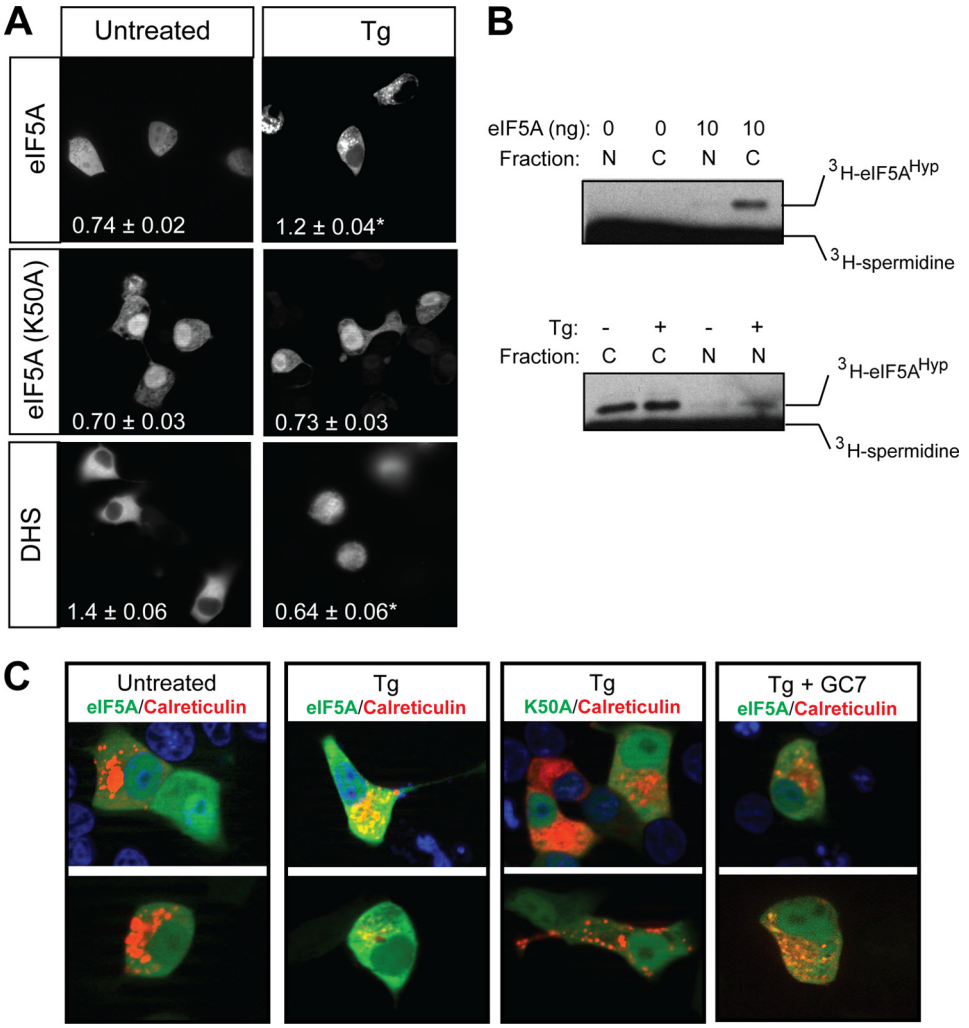

FIGURE 6. **Intracellular localization of eIF5A and DHS in response to Tg-induced ER stress.** *A*, INS-1 (832/13) β cells were transfected with expression vectors encoding GFP-eIF5A, GFP-eIF5A(K50A), or GFP-DHS, and 24 h later were treated with Tg (1 μM) for 4 h. Images shown are representative live cell images (original magnification, ×400) taken in the *green* channel (488 nm excitation). *Numbers in the lower left corner of each panel* represent the cytoplasmic:nuclear ratio of green intensity from at least 10 cells, and an *asterisk* indicates that the number is statistically different ($p < 0.05$) from untreated cells. *B*, results of hypusination assays *in vitro* using recombinant eIF5A protein, [^{3}H]spermidine, and cytoplasmic (*C*) or nuclear (*N*) extracts from INS-1 (832/13) cells. Labeling on the *right* indicates the positions of [^{3}H]eIF5A^{Hyp} and unincorporated [^{3}H]spermidine. *C*, representative images (original magnification, ×630) of INS-1 (832/13) β cells transfected with RFP-calreticulin and either GFP-eIF5A or GFP-eIF5A(K50A) and then counterstained with DAPI (*upper row* only). 24 h after transfection, cells were imaged in the *green* (488 nm excitation), *red* (580 nm excitation), and *blue* (DAPI, 365 nm excitation) channels and then merged. *Upper* and *lower rows* in *C* represent different cells viewed from separate transfections.

and function and significantly improves glucose tolerance (33).

To investigate the molecules that contribute to ER stress in islets, we initially studied *db/db* mice on two different backgrounds: *C57BLKS/J* and *C57BL6/J*. On the *C57BL6/J* background, which is resistant to diabetes and islet dysfunction, we observed that hypusination activity in islets is down-regulated relative to lean (*db/+*) littermate controls, whereas on the *C57BLKS/J* background (which develops diabetes and islet dysfunction), hypusine formation continues unmitigated. This finding suggested to us that persistent hypusination by the rate-limiting enzyme DHS may contribute to islet dysfunction on the *C57BLKS/J* model. Hypusine is an amino acid that is formed post-translationally in a reaction involving the enzymes DHS and deoxyhypusine hydroxylase and the substrates NAD^+ and spermidine and is unique to the protein eIF5A (40). Importantly, hypusine is required for the majority of functions of eIF5A that have been studied to date (41, 42), including those relevant to cytokine-induced β cell dysfunction (13). The relationship between cytokine signaling and incident ER stress (37, 38) therefore led us to investigate whether DHS inhibition in the *C57BLKS/J-db/db* strain might lead to improved glucose homeostasis. For these studies, we used GC7, a spermidine analog that was shown in structural and biochemical analyses to specifically occupy and inhibit the active site of the DHS enzyme (43). Our data presented here show that a 2-week treatment with GC7 leads to significant improvements in fasting glucose levels, glucose tolerance, insulin secretion, proinsulin:insulin ratios, and β cell mass in *C57BLKS/J-db/db* mice. We recognize that because the animals received systemic GC7, we cannot fully rule out the possibility that the effects on insulin secretion and β cell mass were secondary to effects on other tissues (such as muscle, adipose, and

brain). Nonetheless, we observed no differences in food intake, weight, or insulin tolerance during this short treatment period, so significant effects on peripheral tissues and brain seem less likely.

To clarify the direct effects of DHS inhibition on β cell function in the setting of ER stress, we studied INS-1 (832/13) β cells that were induced by Tg to activate the UPR. Interestingly, Tg treatment increases hypusination activity in these cells without any discernible increase in DHS protein levels, and concurrent treatment with GC7 prevents this increase. Although this finding suggests post-translational regulation of DHS activity, we cannot exclude the possibility that Tg might additionally affect the activity or level of the second (nonrate-determining) enzyme of hypusination, deoxyhypusine hydroxylase. We show that the effects of Tg on INS-1 (832/13) β cells recapitulate the changes seen in the UPR, including eIF2-α phosphorylation, CHOP induction, *Xbp1* mRNA splicing, impairments in proinsulin to insulin processing, caspase-3 activation, and apoptosis. Inhibition of DHS by GC7 does not appear to affect certain characteristics of the UPR, such as eIF2-α phosphorylation, *Chop* mRNA induction, or *Xbp1* mRNA splicing, but induction of CHOP and its deleterious downstream effects such as caspase-3 cleavage and apoptosis are inhibited. Notably, some of the protective gene responses, such as activation of antioxidative genes appears unchanged in the setting of DHS inhibition. These findings parallel the results seen in the setting of *Chop* gene deletion in the *db/db* mouse (33) and serve to reinforce the concept that CHOP may be pivotal to cellular execution in the setting of ER stress (38).

The mechanism of CHOP inhibition by GC7 may be related to the known functions of eIF5A^{Hyp}. In this context, recent studies suggest a role for eIF5A^{Hyp} in translational elongation (35), but unlike general translational factors, eIF5A^{Hyp} appears to be responsible for only ~5% of total protein synthesis in unstressed mammalian cells (34). In recent studies, we showed that under conditions of acute cytokine-mediated stress *in vivo* and *in vitro*, eIF5A is necessary for the translation of *Nos2* mRNA and the consequent dysfunction of the islet (13). This translational effect of eIF5A^{Hyp} may be attributable both to the shuttling of the *Nos2* mRNA from the nucleus to the cytoplasm and to enabling its translational elongation at ribosomes. Similarly, under conditions of antigen exposure, eIF5A^{Hyp} is required for the translation of the mRNA encoding the maturation marker CD83 in antigen presenting cells (19). These findings lead us to believe that eIF5A^{Hyp} may be positioned as a stress-responsive factor, enabling the translation of a subset of stress-responsive proteins. In the setting of ER stress, protein translation in the cytosol is acutely inhibited, whereas translation at ER-based ribosomes persists. The mRNAs that continue to be translated in the setting of ER stress appear to localize to these ER-bound ribosomes (36). Our studies of DHS inhibition in the setting of ER stress suggest that eIF5A^{Hyp} may participate in translation at these ER-bound ribosomes, based on co-immunofluorescence of GFP-eIF5A with RFP-calreticulin.

One of the proteins acutely translated in response to the UPR (downstream of ATF4) is CHOP. Despite a 20-fold activation of *Chop* mRNA, CHOP production was suppressed when cells were co-incubated with GC7. By contrast, GC7 did not suppress either *Atf4* mRNA or protein production. Thus, *Chop* mRNA translation may specifically require eIF5A^{Hyp}. We acknowledge that our data do not imply exclusivity regarding translation of *Chop*, and it remains possible that translation of other transcripts, particularly during more prolonged periods of ER stress, are also affected by DHS inhibition. Interestingly, DHS inhibition by GC7 has been shown to block translational elongation (tracking closely with the known actions of eIF5A^{Hyp}) for up to 48 h of incubation in cell culture (34), but for more prolonged periods (≥72 h), it has been reported to impair both translational elongation and initiation (44). This latter effect could represent an "off target" action of GC7, or instead reflect an as yet unidentified role of polyamines and DHS in long term translation. Whereas these long term effects may not be relevant to our studies *in vitro* in β cells, our results using GC7 in *db/db* animals *in vivo* might reflect effects on both translational elongation and initiation.

Taken together, our results identify a potential role for DHS in the maintenance of ER stress. An interesting outcome in our studies was the finding that the compartmentation of DHS may be regulated during ER stress, such that it translocates from the cytoplasm to the nucleus, presumably to catalyze hypusination of a nuclear species of eIF5A. It is tempting to speculate that this translocation process is mediated by post-translational modifications, particularly because DHS contains putative mitogen-activated protein kinase target sites and 14–3-3 recognition sequences, making it possible that post-translational modifications and/or protein chaperones mediate the translocation of DHS during acute stress. We believe that the role of DHS, as with all highly conserved proteins and pathways, must be considered in the context of the specific cell type and underlying physiologic process. In the setting of insulin resistance and its accompanying β cell stress, it is possible that hypusination activity within the islet needs to be down-regulated so as to minimize apoptosis and preserve glycemic control, as observed in the obese, diabetes-resistant *C57BL6/J-db/db* mice. However, precisely how DHS inhibition in the longer term might affect nonislet tissues is unclear at this point. Thus, our studies point to DHS as a target for the treatment of diabetes, but further studies are clearly warranted.

Acknowledgments—We acknowledge the assistance of M. Ryu and N. Stull in islet isolations.

REFERENCES

1. Bergman, R. N., Kim, S. P., Hsu, I. R., Catalano, K. J., Chiu, J. D., Kabir, M., Richey, J. M., and Ader, M. (2007) *Am. J. Med.* **120,** S3–8
2. McGarry, J. D. (2002) *Diabetes* **51,** 7–18
3. Ritchie, S. A., and Connell, J. M. (2007) *Nutr. Metab. Cardiovasc. Dis.* **17,** 319–326
4. Mokdad, A. H., Ford, E. S., Bowman, B. A., Dietz, W. H., Vinicor, F., Bales, V. S., and Marks, J. S. (2003) *JAMA* **289,** 76–79
5. Kahn, S. E., Hull, R. L., and Utzschneider, K. M. (2006) *Nature* **444,** 840–846
6. Sladek, R., Rocheleau, G., Rung, J., Dina, C., Shen, L., Serre, D., Boutin, P., Vincent, D., Belisle, A., Hadjadj, S., Balkau, B., Heude, B., Charpen-

tier, G., Hudson, T. J., Montpetit, A., Pshezhetsky, A. V., Prentki, M., Posner, B. I., Balding, D. J., Meyre, D., Polychronakos, C., and Froguel, P. (2007) *Nature* **445,** 881–885
7. Tabák, A. G., Jokela, M., Akbaraly, T. N., Brunner, E. J., Kivimäki, M., and Witte, D. R. (2009) *Lancet* **373,** 2215–2221
8. Butler, A. E., Janson, J., Bonner-Weir, S., Ritzel, R., Rizza, R. A., and Butler, P. C. (2003) *Diabetes* **52,** 102–110
9. Ogihara, T., and Mirmira, R. G. (2010) *J. Diab. Invest.* **1,** 123–133
10. Prentki, M., and Nolan, C. J. (2006) *J. Clin. Invest.* **116,** 1802–1812
11. Evans-Molina, C., Robbins, R. D., Kono, T., Tersey, S. A., Vestermark, G. L., Nunemaker, C. S., Garmey, J. C., Deering, T. G., Keller, S. R., Maier, B., and Mirmira, R. G. (2009) *Mol. Cell. Biol.* **29,** 2053–2067
12. Tanaka, Y., Gleason, C. E., Tran, P. O., Harmon, J. S., and Robertson, R. P. (1999) *Proc. Natl. Acad. Sci. U.S.A.* **96,** 10857–10862
13. Maier, B., Ogihara, T., Trace, A. P., Tersey, S. A., Robbins, R. D., Chakrabarti, S. K., Nunemaker, C. S., Stull, N. D., Taylor, C. A., Thompson, J. E., Dondero, R. S., Lewis, E. C., Dinarello, C. A., Nadler, J. L., and Mirmira, R. G. (2010) *J. Clin. Invest.* **120,** 2156–2170
14. Moore, C. C., Martin, E. N., Lee, G., Taylor, C., Dondero, R., Reznikov, L. L., Dinarello, C., Thompson, J., and Scheld, W. M. (2008) *J. Infect. Dis.* **198,** 1407–1414
15. Park, M. H., Nishimura, K., Zanelli, C. F., and Valentini, S. R. (2010) *Amino Acids* **38,** 491–500
16. Chatterjee, I., Gross, S. R., Kinzy, T. G., and Chen, K. Y. (2006) *Mol. Genet. Genomics* **275,** 264–276
17. Elfgang, C., Rosorius, O., Hofer, L., Jaksche, H., Hauber, J., and Bevec, D. (1999) *Proc. Natl. Acad. Sci. U.S.A.* **96,** 6229–6234
18. Hauber, I., Bevec, D., Heukeshoven, J., Krätzer, F., Horn, F., Choidas, A., Harrer, T., and Hauber, J. (2005) *J. Clin. Invest.* **115,** 76–85
19. Kruse, M., Rosorius, O., Krätzer, F., Bevec, D., Kuhnt, C., Steinkasserer, A., Schuler, G., and Hauber, J. (2000) *J. Exp. Med.* **191,** 1581–1590
20. Hohmeier, H. E., Mulder, H., Chen, G., Henkel-Rieger, R., Prentki, M., and Newgard, C. B. (2000) *Diabetes* **49,** 424–430
21. Gotoh, M., Ohzato, H., Porter, J., Maki, T., and Monaco, A. P. (1990) *Horm. Metab. Res. Suppl.* **25,** 10–16
22. Dignam, J. D., Lebovitz, R. M., and Roeder, R. G. (1983) *Nucleic Acids Res.* **11,** 1475–1489
23. Iype, T., Francis, J., Garmey, J. C., Schisler, J. C., Nesher, R., Weir, G. C., Becker, T. C., Newgard, C. B., Griffen, S. C., and Mirmira, R. G. (2005) *J. Biol. Chem.* **280,** 16798–16807
24. Lipson, K. L., Fonseca, S. G., Ishigaki, S., Nguyen, L. X., Foss, E., Bortell, R., Rossini, A. A., and Urano, F. (2006) *Cell. Metab.* **4,** 245–254
25. Leiter, E. H., Coleman, D. L., and Hummel, K. P. (1981) *Diabetes* **30,** 1029–1034
26. Baetens, D., Stefan, Y., Ravazzola, M., Malaisse-Lagae, F., Coleman, D. L., and Orci, L. (1978) *Diabetes* **27,** 1–7
27. Laedtke, T., Kjems, L., Pørksen, N., Schmitz, O., Veldhuis, J., Kao, P. C., and Butler, P. C. (2000) *Am. J. Physiol. Endocrinol. Metab.* **279,** E520–528
28. Hostens, K., Pavlovic, D., Zambre, Y., Ling, Z., Van Schravendijk, C., Eizirik, D. L., and Pipeleers, D. G. (1999) *J. Clin. Invest.* **104,** 67–72
29. Ehses, J. A., Lacraz, G., Giroix, M. H., Schmidlin, F., Coulaud, J., Kassis, N., Irminger, J. C., Kergoat, M., Portha, B., Homo-Delarche, F., and Donath, M. Y. (2009) *Proc. Natl. Acad. Sci. U.S.A.* **106,** 13998–14003
30. Lebrun, P., Cognard, E., Gontard, P., Bellon-Paul, R., Filloux, C., Berthault, M. F., Magnan, C., Ruberte, J., Luppo, M., Pujol, A., Pachera, N., Herchuelz, A., Bosch, F., and Van Obberghen, E. (2010) *Diabetologia* **53,** 1935–1946
31. Zhu, X., Zhou, A., Dey, A., Norrbom, C., Carroll, R., Zhang, C., Laurent, V., Lindberg, I., Ugleholdt, R., Holst, J. J., and Steiner, D. F. (2002) *Proc. Natl. Acad. Sci. U.S.A.* **99,** 10293–10298
32. Roe, M. W., Philipson, L. H., Frangakis, C. J., Kuznetsov, A., Mertz, R. J., Lancaster, M. E., Spencer, B., Worley, J. F., 3rd, and Dukes, I. D. (1994) *J. Biol. Chem.* **269,** 18279–18282
33. Song, B., Scheuner, D., Ron, D., Pennathur, S., and Kaufman, R. J. (2008) *J. Clin. Invest.* **118,** 3378–3389
34. Li, C. H., Ohn, T., Ivanov, P., Tisdale, S., and Anderson, P. (2010) *PLoS One* **5,** e9942
35. Saini, P., Eyler, D. E., Green, R., and Dever, T. E. (2009) *Nature* **459,** 118–121
36. Stephens, S. B., Dodd, R. D., Brewer, J. W., Lager, P. J., Keene, J. D., and Nicchitta, C. V. (2005) *Mol. Biol. Cell* **16,** 5819–5831
37. Chambers, K. T., Unverferth, J. A., Weber, S. M., Wek, R. C., Urano, F., and Corbett, J. A. (2008) *Diabetes* **57,** 124–132
38. Shao, C., Lawrence, M. C., and Cobb, M. H. (2010) *J. Biol. Chem.* **285,** 19710–19719
39. Scheuner, D., and Kaufman, R. J. (2008) *Endocr. Rev.* **29,** 317–333
40. Wolff, E. C., Wolff, J., and Park, M. H. (2000) *J. Biol. Chem.* **275,** 9170–9177
41. Lipowsky, G., Bischoff, F. R., Schwarzmaier, P., Kraft, R., Kostka, S., Hartmann, E., Kutay, U., and Görlich, D. (2000) *EMBO J.* **19,** 4362–4371
42. Xu, A., and Chen, K. Y. (2001) *J. Biol. Chem.* **276,** 2555–2561
43. Umland, T. C., Wolff, E. C., Park, M. H., and Davies, D. R. (2004) *J. Biol. Chem.* **279,** 28697–28705
44. Landau, G., Bercovich, Z., Park, M. H., and Kahana, C. (2010) *J. Biol. Chem.* **285,** 12474–12481